Generalized Eady Waves with Ekman Pumping

GARETH P. WILLIAMS AND JOHN B. ROBINSON

Geophysical Fluid Dynamics Laboratory/NOAA, Princeton University, Princeton, N. J. 08540

(Manuscript received 19 March 1974)

ABSTRACT

The effects of Ekman layers on generalized Eady waves (i.e., height-varying static stability and shear) are examined. The non-constancy of $N(z)$ and u_z modify the classical Eady results but do not introduce any new effects. Thus, a short-wave cutoff is always found for flows with double Ekman layers but never for flows with a single Ekman layer.

By comparing the analytical solutions with a numerically simulated annulus wave, we are able to categorize the latter quite accurately.

1. Introduction

The baroclinic waves that occur in laboratory annulus experiments are thought to be essentially Eady-type waves. There are, however, two major modifying influences that alter the classical Eady description. These are the effects produced by Ekman layer friction and by the vertical variation in the static stability. The separate influence of each of these factors on baroclinic waves has been studied by Barcilon (1964) for the double Ekman layer effect and by Williams (1974) for the static stability effect.

In this paper we examine the influence of the combined processes of static-stability-shear variation and Ekman layer friction on baroclinic waves and use the results to analyze the annulus waves. This is done by comparing the phase-amplitude distributions of the theoretical solutions with those of a numerically simulated annulus wave. This differs from the customary procedure of comparing stability transition curves.

2. Mathematical formulation

The formulation of the baroclinic instability problem is well-known. The extension of Eady's analysis to cover the case of mutually height-varying static stability and shear has been given by Williams (1974), referred to hereafter as W. We will draw on that paper in outlining the following formulation.

We consider small-amplitude, inviscid adiabatic perturbations to a parallel flow, $u(y,z)$, in the x direction of a channel limited by boundaries at $z=0$, H and $y=0$, L on which the normal velocities must vanish. The Cartesian coordinates (x,y,z) are in a frame of reference rotating about the vertical z axis with angular velocity $f/2$. We take $\mathcal{S}_\epsilon$ and $\mathcal{N}_\epsilon$ to be characteristic values of the shear u_z (a frequency) and of the gravitational (Brunt-Väisälä) frequency $N(z)=(\beta g dT_s/dz)^{\frac{1}{2}}$ for a stably stratified Boussinesq fluid. The subscript ϵ denotes, for reasons that will become apparent, the non-constancy of these frequencies with respect to z.

For this particular baroclinic instability problem the following scaling is most appropriate:

$$\left.\begin{array}{ll} \mathcal{N}_\epsilon H/f & \text{the horizontal coordinates } (x,y) \\ H & \text{the vertical coordinate } z \\ \mathcal{N}_\epsilon/(f\mathcal{S}_\epsilon) & \text{the time } t \\ \mathcal{S}_\epsilon H & \text{the horizontal velocities } (u,v) \\ f H \mathrm{R}_\epsilon^2 & \text{the vertical velocity } w \\ H^2\mathcal{N}_\epsilon\mathcal{S}_\epsilon & \text{the Boussinesq pressure } p/\rho \\ H\mathcal{N}_\epsilon\mathcal{S}_\epsilon & \text{the Boussinesq buoyancy } \sigma[=-\beta g T] \end{array}\right\}. \quad (1)$$

In the quasi-static, quasi-geostrophic state the Rossby-Kibel number $\mathrm{R}_\epsilon \approx \mathcal{S}_\epsilon/\mathcal{N}_\epsilon$ (being the reciprocal of the square root of the Richardson number) is small and the governing equations are those for the conservation of quasi-geostrophic potential vorticity, q, and for the advection of buoyancy, σ. When these equations are linearized to describe normal-mode perturbations of the basic state, they can be written, on transposing all the variables [except $N(z)$] to nondimensional form, as

$$\hat{q} + (u-c)^{-1} q_y \hat{\psi} = 0, \quad (2)$$

$$\hat{q} = (\mathrm{F}\hat{\psi}_z)_z + \hat{\psi}_{yy} - \alpha^2\hat{\psi}, \quad (3)$$

$$q_y = -(\mathrm{F}u_z)_z - u_{yy}, \quad (4)$$

$$\hat{w} = i\alpha\mathrm{F}[u_z\hat{\psi} - (u-c)\hat{\psi}_z], \quad (5)$$

where $\hat{q}$, $\hat{\psi}$, $\hat{w}$ are the complex amplitude functions for a perturbation of the form $\psi = \mathrm{Re}\hat{\psi}(y,z)e^{i\alpha(x-ct)}$. The nondimensional wavenumber α is a real variable whereas the nondimensional phase velocity $c=c_r+ic_i$ can be complex. The streamfunction ψ for the dimensionless horizontal velocities is also the quasi-geostrophic pressure whereas its gradient ψ_z, by virtue of the hydrostatic relation $\sigma=-\psi_z$, describes the quasi-geostrophic

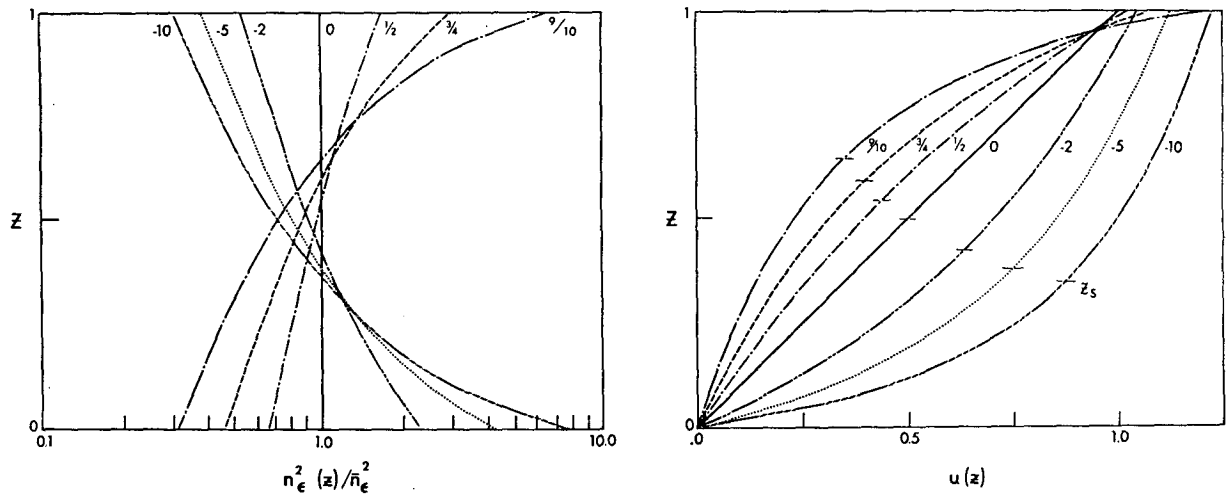

FIG. 1. Associated distributions of the normalized static-stability-shear function $\bar{n}_\epsilon^2(z)=(1-\epsilon z)^{-4/3}/\bar{n}_\epsilon^2$, and the nondimensional mean flow $u(z)$ [Eq. (9)], with intercepts indicating the steering level z_s of inviscid waves, for values of ϵ as indicated.

temperature. The parameter $F(z)=\mathfrak{N}_\epsilon^2/N^2(z)$ is the basic baroclinic instability parameter, sometimes called the rotational Froude number.

For the problem in hand u is assumed to be independent of the lateral coordinate y so that q_y is independent of y, and solutions of the form $\hat{\psi}(y,z)=\hat{\psi}(z)\sin my$ exist to satisfy the lateral boundary conditions. To eliminate the term in $(u-c)^{-1}$ we make the generalized Eady constraint (see W) that the product Fu_z be constant.[1] To achieve this the z variability of the basic state is taken to be of a form

$$N(z)=\mathfrak{N}_0 n_\epsilon(z), \quad u_z^d(z)=\mathcal{S}_0 s_\epsilon(z),$$

such that $n_\epsilon^2(z)=s_\epsilon(z)$, i.e., the vertical and horizontal density variations are *non-uniform*. The dimensional and nondimensional shears are, u_z^d and $u_z=u_z^d/\mathcal{S}_\epsilon$, respectively. Following W, the characteristic frequencies are based on integral forms such that

$$\frac{\mathfrak{N}_\epsilon^2}{\mathfrak{N}_0^2}=\frac{\mathcal{S}_\epsilon}{\mathcal{S}_0}=\bar{n}_\epsilon^2, \tag{6}$$

where $\bar{n}_\epsilon$ is the integral of the distribution function $n_\epsilon(z)$ over $z=0$, 1; and $\mathfrak{N}_0$ and $\mathcal{S}_0$ are the characteristic frequencies of the uniform (Eady) basic state. Introducing the normalized distribution function $\bar{n}_\epsilon(z)=n_\epsilon(z)/\bar{n}_\epsilon$, Eq. (6) allows us to write $u_z=\bar{n}_\epsilon^2(z)$ and $F(z)=u_z^{-1}$. The equation for the conservation of potential vorticity in the fluid interior then reduces to

$$\left(\frac{\hat{\psi}_z}{\bar{n}_\epsilon^2(z)}\right)_z=K^2\hat{\psi}, \tag{7}$$

where $K^2=4k^2=\alpha^2+m^2$.

Finally, we assume that the predominant role of friction is in producing Ekman layer pumping—this is correct to $O(E^{\frac{1}{2}})$, i.e., when the Ekman layers are of infinitesimal thickness. The pumping of these Ekman layers produces vertical velocities $w=(\pm)(E/R_\epsilon)^{\frac{1}{2}}\zeta$ on $z=\binom{0}{1}$, respectively, where ζ is the vertical component of vorticity. Combining with (5) this provides boundary conditions on $\hat{\psi}$ which can be written:

$$\hat{\psi}u_z\left[1+i\left\{\begin{smallmatrix}+Q_1\\-Q_0\end{smallmatrix}\right\}\right]-(u-c)\hat{\psi}_z=0, \quad \text{on } z=\left\{\begin{smallmatrix}1\\0\end{smallmatrix}\right\}, \tag{8}$$

where $Q=K\tilde{Q}=(K^2/\alpha)(E/R_\epsilon)^{\frac{1}{2}}$ is the basic parameter of this problem with $E=\nu/(2fH^2)$ being an Ekman number. The suffices on Q in (8) are traces that allow us to consider either single or double Ekman layer flows by separate specification. A formal derivation of the $O(E^{\frac{1}{2}})$ equations has been given by Pedlosky (1971).

It follows from W that (7) and (8) can be solved for a wide variety of $n_\epsilon(z)$ distributions by using such methods as the WKB technique [see, e.g., Richards (1959, pp. 349–351) for this and other solution types]. However, as in W, attention will be limited to the instructive class of *exact* solutions that are obtainable for the particular distribution $n_\epsilon(z)=(1-\epsilon z)^{-\frac{3}{2}}$, $-\infty<\epsilon<1$. The standard Eady or Barcilon problem corresponds to the case $\epsilon=0$.

3. The eigenvalue solution

For the generalized exact Eady problem we consider the stability of the mean current

$$u(z)=[(1-\epsilon z)^{-\frac{1}{2}}-1]/[\bar{n}_\epsilon^2\epsilon/3], \tag{9}$$

where $\bar{n}_\epsilon=[1-(1-\epsilon)^{\frac{1}{2}}]/[\epsilon/3]$. The form of this flow and the associated normalized static-stability-shear distribution, $\bar{n}_\epsilon(z)$, are shown in Fig. 1 for cases of increasing ($\epsilon>0$) and decreasing ($\epsilon<0$) static-stability-shear. It is the comparative stability of this functionally related family of flows that will be examined. For the moderate ϵ values shown, the mean flows have roughly

[1] It follows below that this constant is unity.

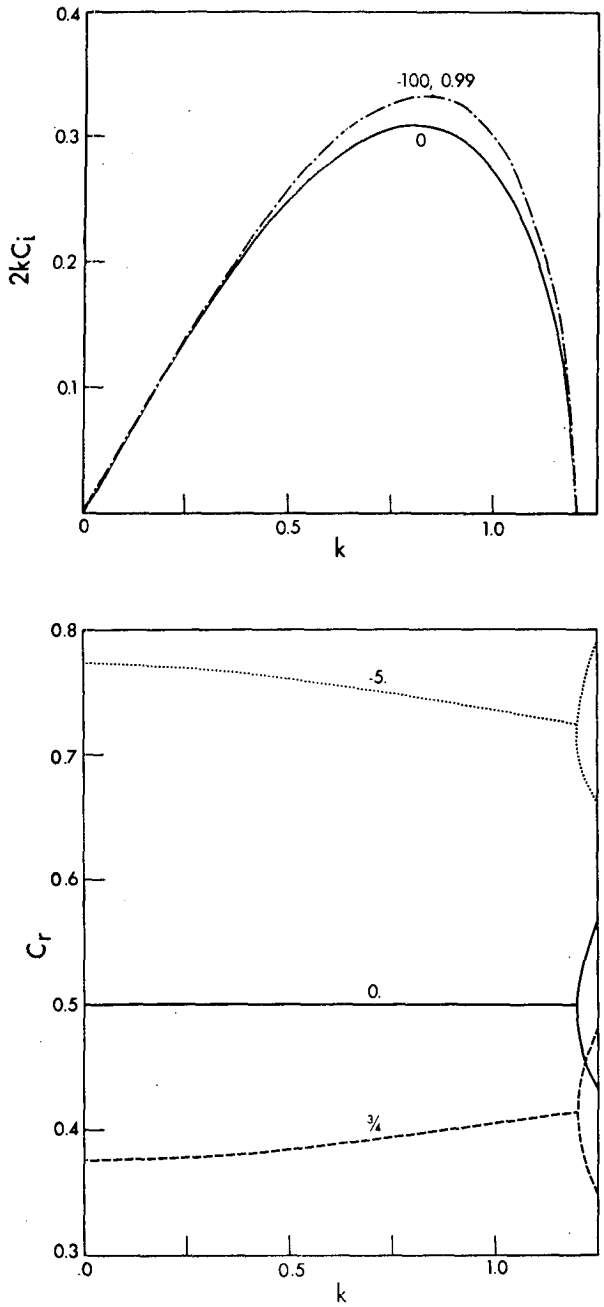

FIG. 2. Variation with wavenumber k of the growth rate $2kc_i$ and phase speed c_r, for values of ϵ as indicated and inviscid waves.

similar maxima so that differences in stability behavior will be due to differences in the *shape* of these profiles.

The solution to (7) and (8) for this set of flows can be written

$$\hat{\psi}(z)=\bar{n}_\epsilon^{\frac{1}{2}}(z)\left\{\frac{Kc}{\bar{n}_\epsilon}\cosh Kn_\epsilon^*(z)-\left[\frac{(1-iQ_0)}{\bar{n}_\epsilon^2}+\frac{\epsilon c}{3}\right]\sinh Kn_\epsilon^*(z)\right\}, \quad (10)$$

where

$$n_\epsilon^*(z)=\int_0^z \bar{n}_\epsilon(z)dz=[1-(1-\epsilon z)^{\frac{1}{3}}]/[1-(1-\epsilon)^{\frac{1}{3}}].$$

Thus, $n_\epsilon^*(1.0)=1.0$.

The corresponding secular equation for the complex wave speed c is most conveniently written as

$$A\tilde{c}^2+B\tilde{c}+C=0, \quad (11)$$

with

$$\left.\begin{aligned} A&=aK^2+(a-1)^2M\\ B&=-K^2-2(a-1)M+iM(aQ_0+a^{-1}Q_1)\\ &\qquad +i(Q_0+Q_1)\\ C&=(1-iQ_0)(M-ia^{-1}Q_1)\end{aligned}\right\},$$

where $M\equiv K\coth(K)-1$, $\tilde{c}=\bar{n}_\epsilon c$, and $a\equiv(1-\epsilon)^{\frac{1}{3}}$. The discriminant $\delta=B^2-4AC$ of this equation is

$$\begin{aligned}\delta=&K^2[K^2-4M]-Q_0^2[1+aM]^2-Q_1^2[1+a^{-1}M]^2\\ &+2Q_0Q_1[2K^2-1-M(M+4-a-a^{-1})]\\ &+2iQ_0[K^2(aM-1)+2(1-a)(M+M^2)]\\ &+2iQ_1[K^2(1-a^{-1}M)+2a^{-1}(1-a)(M+M^2)]. \quad (12)\end{aligned}$$

This quantity is complex for the general case, but reductions are possible and we discuss the important subcases below.

a. *Inviscid waves*

For reference we recall the results obtained in W for generalized Eady flows without Ekman layers. There we showed that (i) unstable waves occur when $k<1.2$ just as in the Eady case, (ii) to a good approximation $c_i=c_{i0}$ for all k, i.e., the growth rate is the same as in the $\epsilon=0$ (Eady) case, and (iii) the fastest growing wave moves with the speed $c_r=u(z_s)$, where the steering level z_s $[=(1-\bar{n}_\epsilon^{-2})/\epsilon]$ is defined as being the height where $\bar{n}_\epsilon(z_s)=1$ (see Fig. 1). The simple Eady type results in (i) and (ii) are due to (and are the reason for) the choice in (6) of scaling factors for $\mathfrak{N}_\epsilon$ and $\mathcal{S}_\epsilon$, respec-

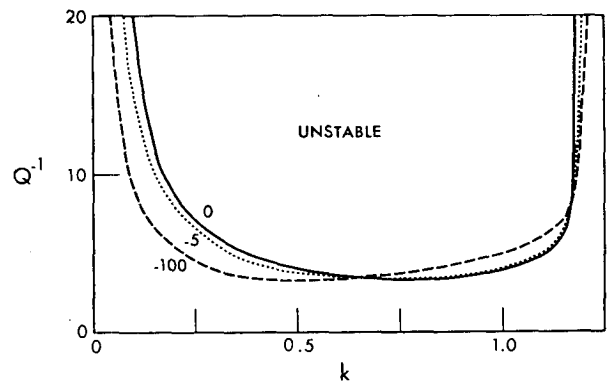

FIG. 3. Double Ekman case: instability transition curve as a function of Q^{-1} for ϵ as shown and $m=0$. Unstable region lies above curve.

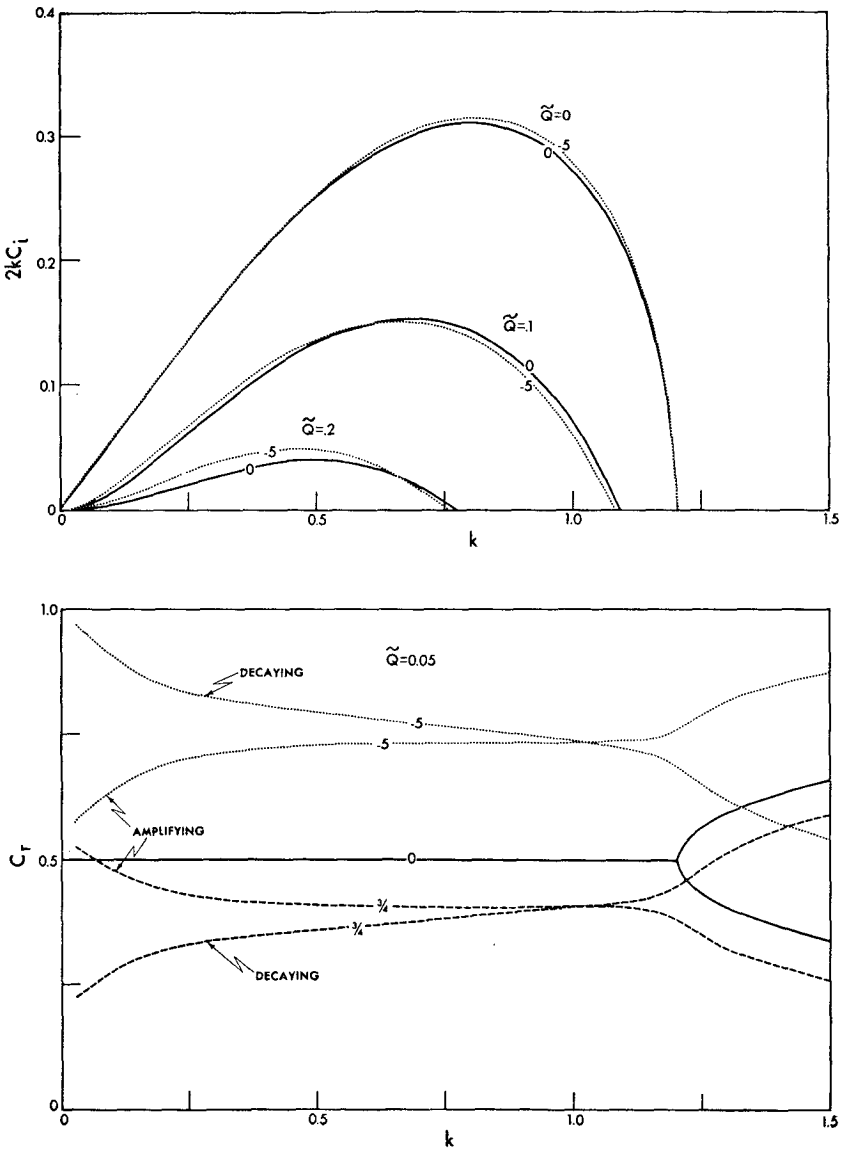

FIG. 4. Double Ekman case: variation with k of growth rate and phase speed for ϵ and $\tilde{Q}$ as shown.

tively. Thus, all the flows in Fig. 1 produce waves with the same growth rate despite their different shapes. The difference in profiles, however, does affect the wave speed c_r which is given by the mean flow speed at the height at which $N(z)$ is equal to its mean value. Thus, the $\epsilon<0$ profiles have the larger phase speeds. These results are summarized by Fig. 2 which shows the growth rate and phase speed for all k. Extreme ϵ are needed to display differences in c_i from the Eady case. The phase speeds are weakly dispersive for $\epsilon\neq 0$ unlike the Eady case.

b. Double Ekman layer case

For Ekman layers of equal strength at $z=0$, 1 we have $Q_0=Q_1=Q$ and the discriminant (12) simplifies. When $\epsilon=0$, the discriminant reduces further and gives the Barcilon (1964) result that onset of instability occurs for a value of Q given by $c_i\to 0$, i.e.,

$$M-k^2=Q^2. \tag{13}$$

For a given value of $Q(k)$ there are two values of k at which transition to instability occurs. These transitions correspond to the upper and lower transition in the annulus experiments. Numerical evaluation of the transition curve for this and $\epsilon\neq 0$ cases (Fig. 3) indicates that ϵ effects appear to be secondary except through the definition of Q which implicity contains an $\bar{n}_\epsilon$ factor.

The double Ekman layers reduce the growth rates and further stabilize the smaller scales for all ϵ as shown

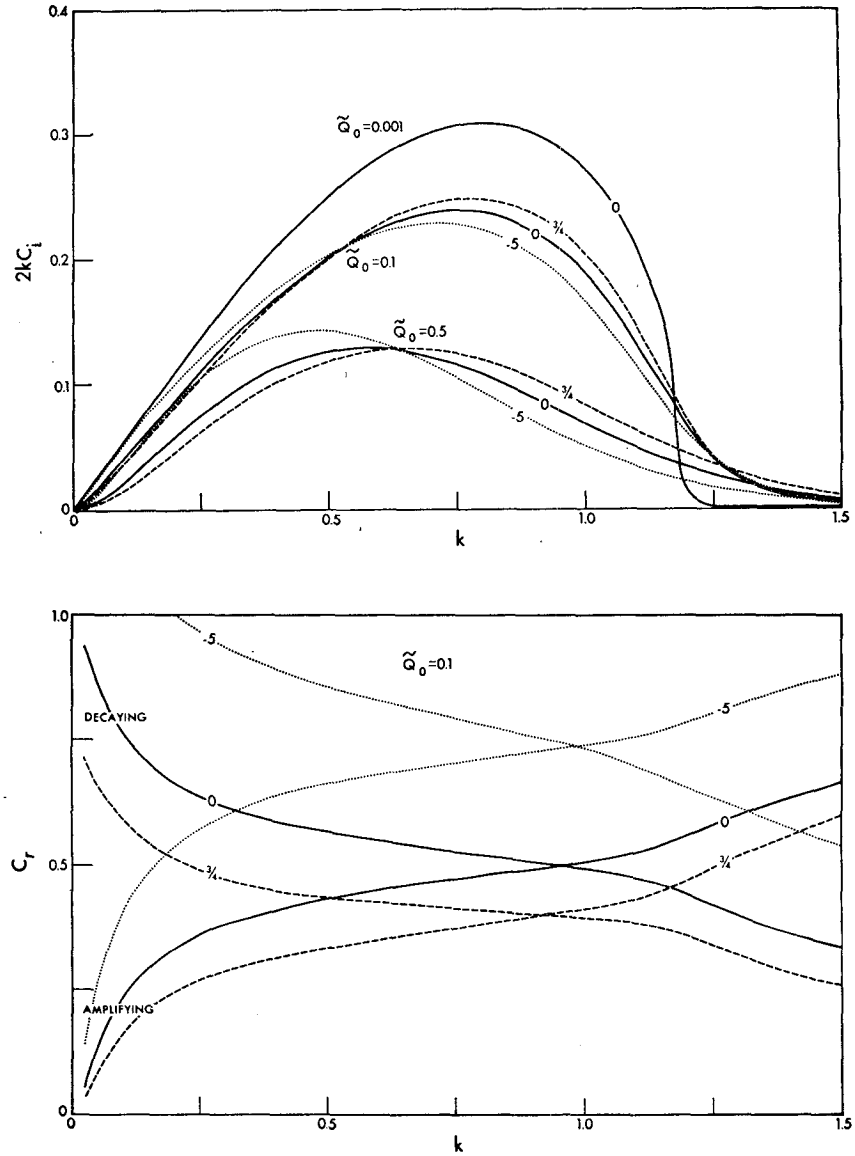

FIG. 5. Single Ekman case: variation with k of growth rate and phase speed for ϵ and $\tilde{Q}_0$ as shown.

in Fig. 4. The cutoffs are sharp. The effect of ϵ on phase speed is more marked, producing two dispersive values of c_r when $\epsilon \neq 0$. The growing waves have faster (slower) phase speeds when $\epsilon > 0$ (< 0) than the damped waves.

c. *Single Ekman layer case*

The eigensolutions for flows with one Ekman layer and one free surface differ appreciably from the double layer case. The growth rates for the single upper or lower layer cases are very similar so we show only the lower case in Fig. 5. This is obtained by setting $Q_0 = Q$, $Q_1 = 0$ in (11) and (12). The most significant features of these growth rates are the moderate ϵ effects and the absence of a short-wave cutoff. Thus even the smallest waves are destabilized, if only weakly so. It can be shown that for c_i to be zero in this case requires

$$Q^2 M[aK^2 + M(1-a)^2][K^2 - \coth^2 K] = 0, \qquad (14)$$

i.e., $K = 0$ or ∞, so there are no meaningful roots. Thus Barcilon's (1964) explanation of the annulus transition diagram does not apply to the free surface experiments.

The wave speeds in Fig. 5 are strongly dispersive even when $\epsilon = 0$. Here there is a difference between the single upper and lower layer case in that growing waves are slower than damped ones for the lower layer case whereas the opposite holds for the upper layer case.

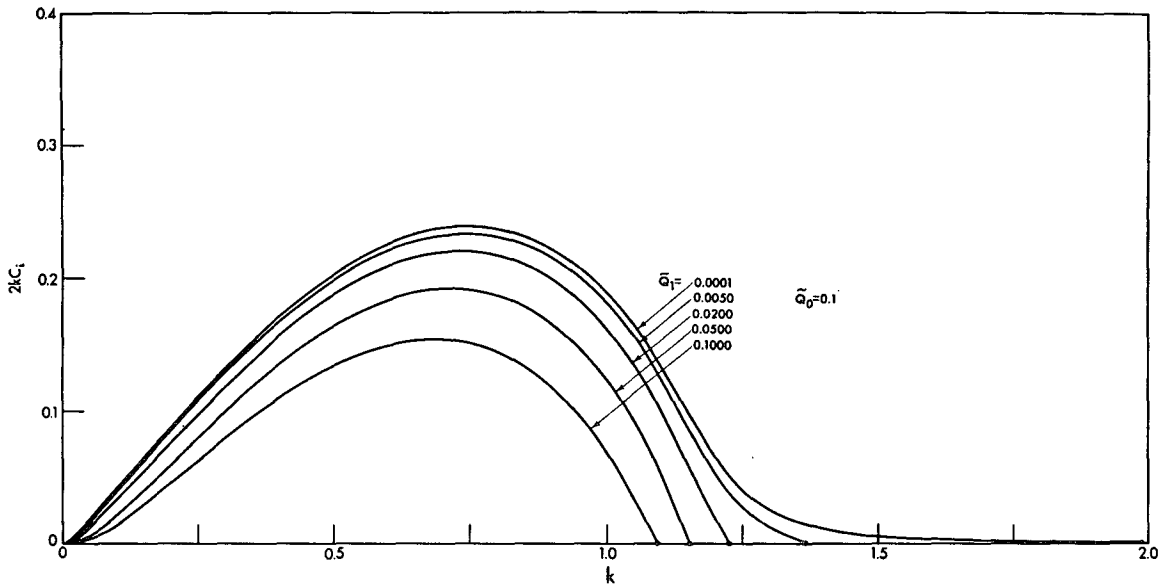

FIG. 6. Unequal Ekman case: variation with k of the growth rate for $\epsilon=0$ for unequal Ekman layers. Primary layer on $z=0$ has $\tilde{Q}_0=0.1$ with miscellaneous secondary layers at $z=1$ having $\tilde{Q}_1=10^{-4}\rightarrow 0.1$ as indicated. Dots denote short-wave cutoffs.

d. Two unequal Ekman layers

The presence of a short-wave cutoff in the double Ekman layer case but its absence in the single Ekman layer case presents something of a paradox, particularly in view of the annulus experiments for which stability transitions are apparent in both cases. Clearly the results must be sensitive to the idealized formulation of friction, particularly for the single Ekman layer case where the $O(E^{\frac{1}{2}})$ equations do not seem to be sufficient to provide the cutoff. To examine this problem further we consider the case of a primary single lower Ekman layer of $\tilde{Q}_0=0.1$ to which is successively added a secondary upper Ekman layer with values of $\tilde{Q}_1$ ranging from 10^{-4} to 0.1; i.e., we examine in effect the transition from the single to the double layer case. The weak additional friction (Fig. 6) is sufficient to produce a cutoff in the instability at values of k close to the values obtained in the double equal Ekman layer case.

It appears from these results that the stability transitions obtained in the free surface annulus experiments must be determined either by the weak Ekman layer at the air-water interface or by the higher order (in E) friction effects in the interior or lower Ekman layer. Such forces are difficult to account for properly. The sensitivity of the cutoff to secondary friction forces shown in Fig. 6 suggests that the transition curves in the free surface experiments may be imprecise.

4. Character of Eady-Ekman and annulus waves

There are many variations to the form of the solution given by (10)–(12). We will present some typical solutions for representative values of Q and ϵ. The reference cases for $Q=0$ are given in W. The stratifications are of the annulus ($\epsilon=-5$) and ocean ($\epsilon=\frac{3}{4}$) types.

a. Double Ekman case

The character of the fastest growing unstable waves for flow with a moderate frictional influence at both surfaces is shown in Fig. 7. The main effect of Ekman pumping is to increase the phase differences in ψ and w_z between the top and bottom of the fluid and to completely alter the w phase distribution near the boundaries where the pumping forces w into phase with ψ. The amplitude of w at the boundaries indicates the strength of the pumping.

b. Single Ekman case

For this type of flow, we can make a comparison with annulus waves by using the data obtained from a numerical integration of the complete Navier-Stokes equations, following Williams (1971). In the numerical solution the parameters had the values $E=3.5\times10^{-4}$, $\mathcal{S}=0.1$ and $\mathfrak{N}=0.5$ in the central annulus region. These give a value of $\tilde{Q}=0.1$ for the pumping parameter. The vertical variation of u_z and $N(z)$ are the same and correspond to an $\epsilon=-4$ distribution [Fig. 4 in Williams (1974)]. Thus, we might expect the annulus waves to be similar to the theoretical solution for $\epsilon=-4$ and $\tilde{Q}_0=0.1$.

In Fig. 8 we make a comparison between the phase and amplitude distributions extracted from the finite-amplitude, equilibrated annulus wave and the appropriate solution given by the above linear theory. The phases are compared as a group by matching the w

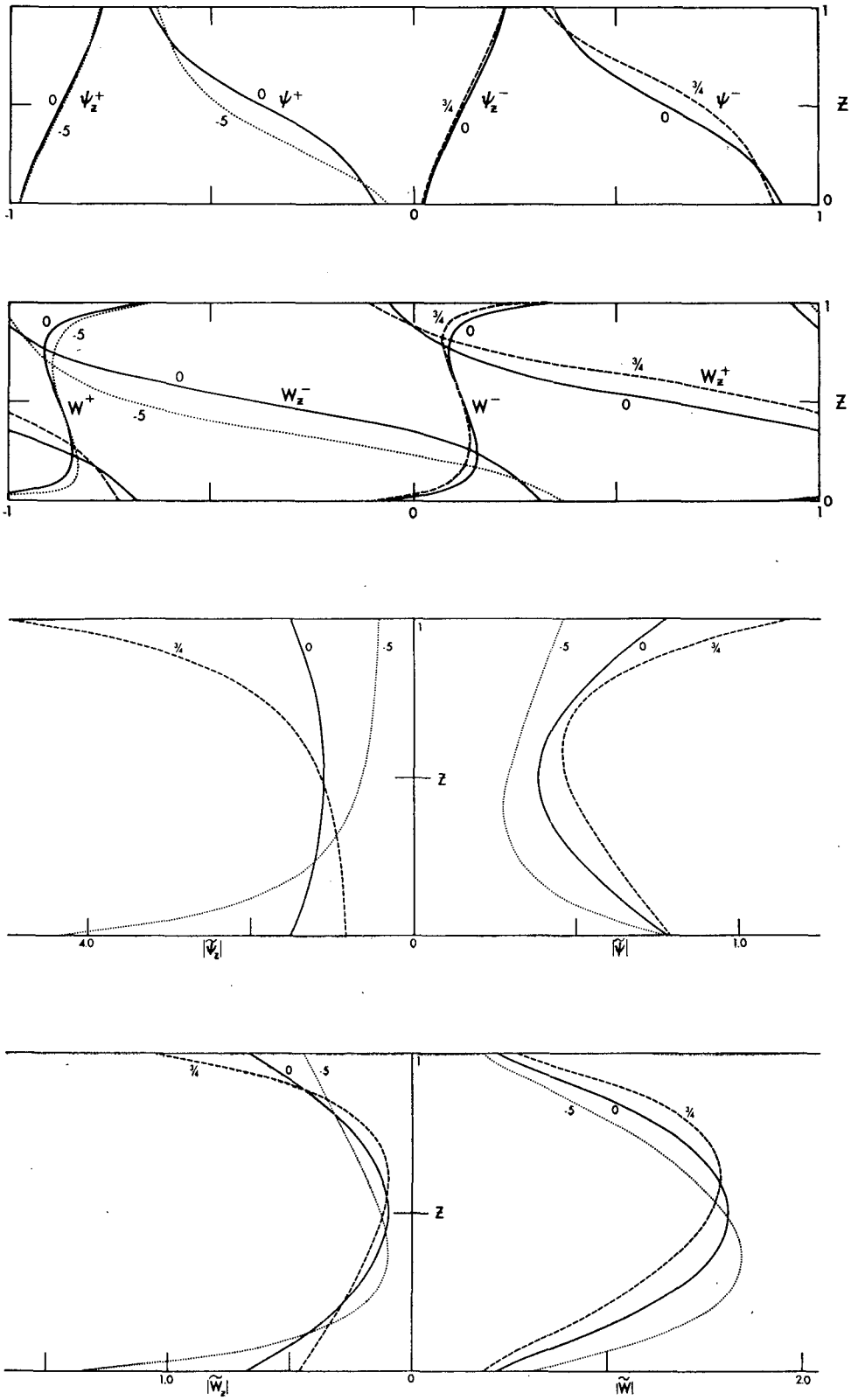

FIG. 7. Double Ekman case: phase and amplitude distributions for most unstable generalized exact Eady-Ekman waves—$k=0.46, 0.50, 0.47$ for $\epsilon=-5, 0, \frac{3}{4}$, respectively, and $\tilde{Q}_0=\tilde{Q}_1=0.05$. Phases, in units of π, are shown for right (left) half of wave when $\epsilon>0$ (<0).

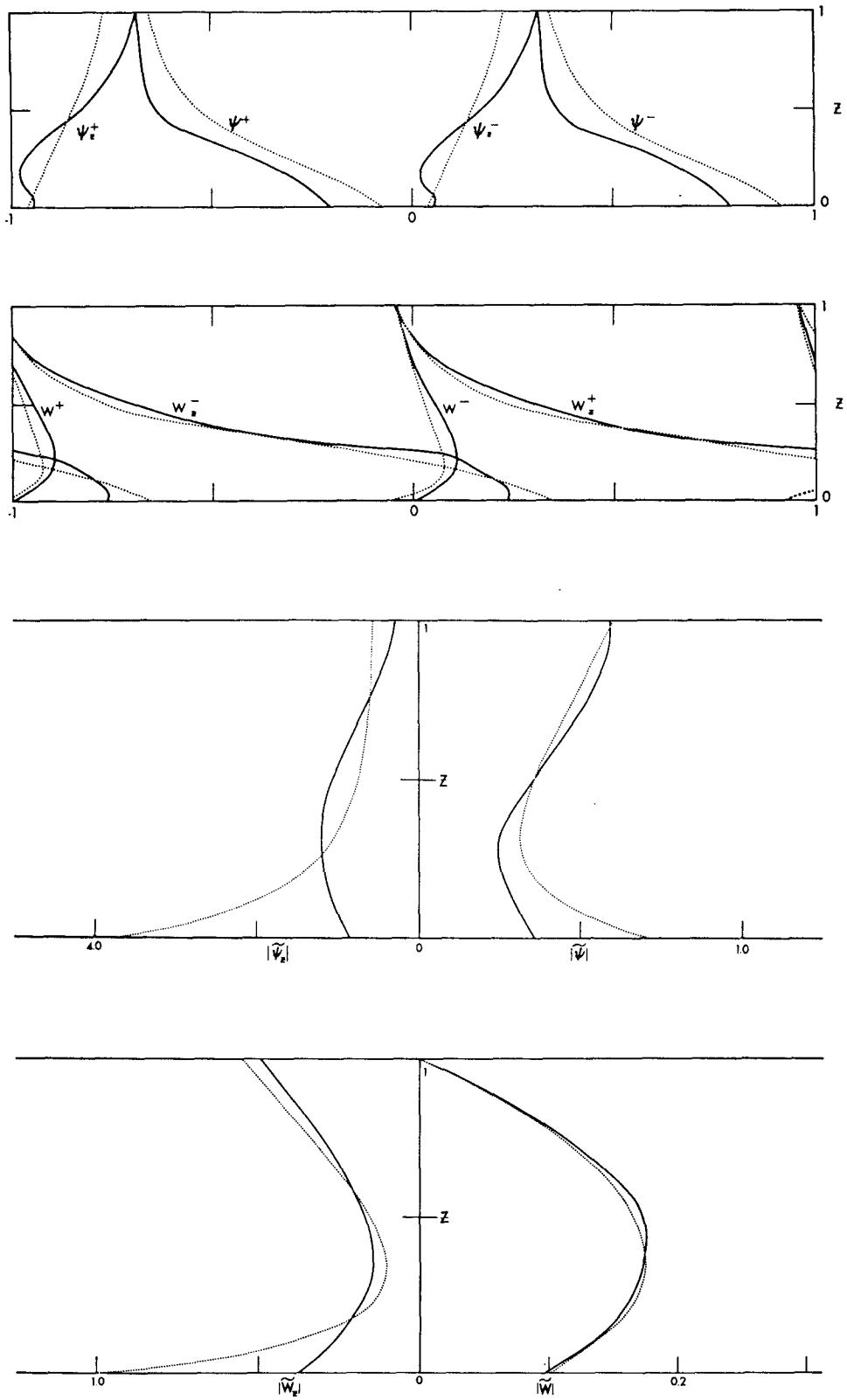

FIG. 8. Single Ekman case: Comparative phase and amplitude distributions of (i) the most unstable generalized Eady-Ekman wave with $\epsilon=-4$ and $\tilde{Q}_0=0.1$ [dotted lines] and (ii) numerical annulus solution at $r'=0.5$ of Williams (1971) [solid lines]. Ekman layer on $z=0$ only.

phases at $z=1$. The amplitudes are arbitrarily scaled to compare shapes only. Comparison of the complete and theoretical solutions indicates a reasonable agreement. The w fields are particularly well represented in phase and amplitude so the Ekman effect is accurately approximated by the pumping formulation. The ψ fields are reasonably similar but there are significant differences in ψ_z. These differences are partly due to the annulus basic state not being identically of the $\epsilon=-4$ type in lower levels but are mainly due to the finite-amplitude configuration of the annulus wave. The temperature field is the most nonlinear annulus field.

Fig. 5 indicates that for this case of $\tilde{Q}=0.1$, the frictional pumping effects are moderate so the wave growth rate is only slightly reduced from its inviscid limit.

Thus, despite the fact that the annulus wave has a complex basic state, a finite amplitude, finite Ekman layers, side walls that limit pumping, and is equilibrated, it nonetheless still possesses many of the characteristics of the unstable waves described by the above $O(E^{\frac{1}{2}})$ linear theory. Improved descriptions would seem to require the inclusion of the effects of finite development.

5. Conclusions

We have reexamined the Eady-Ekman problem allowing for z variations in static stability and shear. This leads to a variety of solution forms about the classical ones but the physics remains basically unaltered, being determined by the constraint $q_y=0$. This class of solutions to the baroclinic instability problem appears to be particularly relevant to the annulus experiments (at least at $r'=0.5$) and a comparison with a complete annulus solution indicates that the annulus waves are essentially a type of Eady wave that has been modified by height-varying static stability and the Ekman layer. The possibility of structural changes in the form of baroclinic waves in the atmosphere could be an important item in climate modeling.

REFERENCES

Barcilon, V., 1964: Role of Ekman layers in the stability of the symmetric regime obtained in a rotating annulus. *J. Atmos. Sci.*, **21**, 291–299.

Pedlosky, J., 1971: Geophysical fluid dynamics. *Mathematical Problems in the Geophysical Sciences*, W. H. Reid, Ed., Providence, R. I., Amer. Math. Soc., 1-60.

Richards, P. I., 1959: *Manual of Mathematical Physics*. New York, Pergamon, 486 pp.

Williams, G. P., 1971: Baroclinic annulus waves. *J. Fluid Mech.*, **49**, 417–449.

——, 1974: Generalized Eady waves. *J. Fluid Mech.*, **62**, 643–655.